AJNR Am J Neuroradiol 24:2015–2019, November/December 2003

Case Report

Serial Proton MR Spectroscopy and Diffusion Imaging Findings in HIV-Related Herpes Simplex Encephalitis

Philipp G. Sämann, Jürgen Schlegel, Georg Müller, Franz Prantl, Christoph Emminger, and Dorothee P. Auer

Summary: We report the case of pathologically proved atypical herpes simplex encephalitis (HSE) in a 40-year-old male patient with AIDS who was followed up by MR imaging, which included diffusion-weighted imaging and proton MR spectroscopy (^{1}H-MRS). MR revealed sparing of hippocampi and limbic cortices, necrosis of both cingulate gyri, and cerebellar involvement. Increased diffusivity and severe metabolic alterations were compatible with biopsy findings of necrotizing inflammation. Clinical recovery corresponded with partial metabolite and diffusion normalization and a myo-inositol increase that indicated evolving gliosis formation further corroborated by immunohistochemistry results. ^{1}H-MRS and diffusion-weighted imaging may both support the diagnosis of HSE in patients with AIDS and help in the follow-up of necrotizing inflammation.

Herpes simplex encephalitis (HSE) associated with HIV infection is a rare complication and may present with atypical clinical and neuropathologic features (1–3). The frequency of HSE in HIV patients with neurologic symptoms was 2% in an autopsy-controlled polymerase chain reaction (PCR) study (3), suggesting a clinicoradiologic underestimation. Moreover, accumulating evidence supports that the neurotoxicity of herpes simplex virus (HSV) and $CD4^+$ T cell–independent immune mechanisms are sufficient to produce various forms of necrotizing extralimbic and classic acute limbic encephalitis in patients with very low $CD4^+$ counts (1–3).

In the diagnostic workup of neurologic complications of HIV infection, MR imaging plays a predominant role. Image interpretation can be difficult, however, because of the frequent coexistence of different pathologic entities, partial overlap of their imaging features, and the infrequent pathologic proof. Proton MR spectroscopy (^{1}H-MRS) and diffusion-weighted imaging have been applied to more common focal HIV-associated brain lesions such as lymphoma, toxoplasmosis, progressive multifocal leukencephalopathy (PML), HIV-related leukencephalopathy, and cryptococcosis. Both techniques reveal supportive information on metabolic changes and tissue integrity, but controversy surrounds their ability to specifically differentiate such lesions (4–6).

To further characterize potential specificities and diagnostic aspects of HSE in HIV, we report unusual neuroradiologic findings in a 40-year-old man with AIDS at CDC stage C3 who was repeatedly studied with MR imaging, including diffusion-weighted imaging and ^{1}H-MRS, throughout the course of HSE which was confirmed at biopsy.

Case Report

The patient was a longstanding intravenous drug abuser who had been diagnosed with HIV 14 years earlier. He presented with a 3-week history of progressive gait imbalance and drowsiness. On admission, he was febrile, somnolent, and disoriented to time and place but able to follow commands; examination disclosed a moderate paresis and hypesthesia of his right leg with hyperactive motor reflexes, a mild paresis of his right arm, and reduced fine motor skills. Plantar reflexes were normal, and there was no evidence of meningismis.

Laboratory findings were remarkable for a $CD4^+$ count of 66/μL and a virus load of 96×10^3 (serum) and 29×10^3 (CSF) HIV RNA copies/mL, respectively. CSF analysis furthermore revealed mild pleocytosis (9/μL, 97% lymphocytes), intrathecal IgG synthesis, and normal levels of glucose, protein, and lactate. Negative findings were obtained for bacteria, fungi, and acid-fast bacilli, cryptococcal antigen, syphilis serology, and PCR for HSV, cytomegalovirus (CMV), JC virus, varizella zoster virus (VZV), and mycobacteria.

MR imaging 4 weeks after the onset of symptoms (Fig 1A and B) showed multifocal confluent lesions that involved both cingulate and parahippocampal gyri, the left anterior capsule, and the body and splenium of the corpus callosum extending bilaterally into the perisplenial white matter. Signal intensity was high on T2-weighted and fluid-attenuated inversion recovery images and markedly reduced on T1-weighted images. Lesion borders were moderately demarcated; no intralesional or meningeal gadolinium enhancement and minimal mass effect were present. Two similar lesions were found in the left occipital and cerebellar subcortical white matter in addition to moderate T2-weighted hyperintensities in both anterior thalami and the right anterior internal capsule. The adjacent cortices were almost completely spared.

^{1}H-MRS of the right perisplenial lesion showed substantially reduced N-acetylaspartate (NAA), markedly elevated lactate (Lac), elevated choline-containing compounds (Cho) and mobile lipids (Lip), normal *myo*-inositol (mI), and slightly reduced total creatine (Cr) (Fig 2A).

Received November 15, 2002; accepted after revision April 21, 2003.

From the Max-Planck-Institute of Psychiatry, NMR Study Group (P.G.S., D.P.A.); Krankenhaus München-Schwabing, Teaching Hospital, Ludwig-Maximilians-Universität; and Department of Neuropathology (J.S.), Departments of Infectious Diseases (G.M., C.E.) and Pathology (F.P.), Technical University of Munich, Munich, Germany.

Address correspondence to PD Dr. Dorothee P. Auer, Kraepelinstraβe 10, 80804 Munich, Germany.

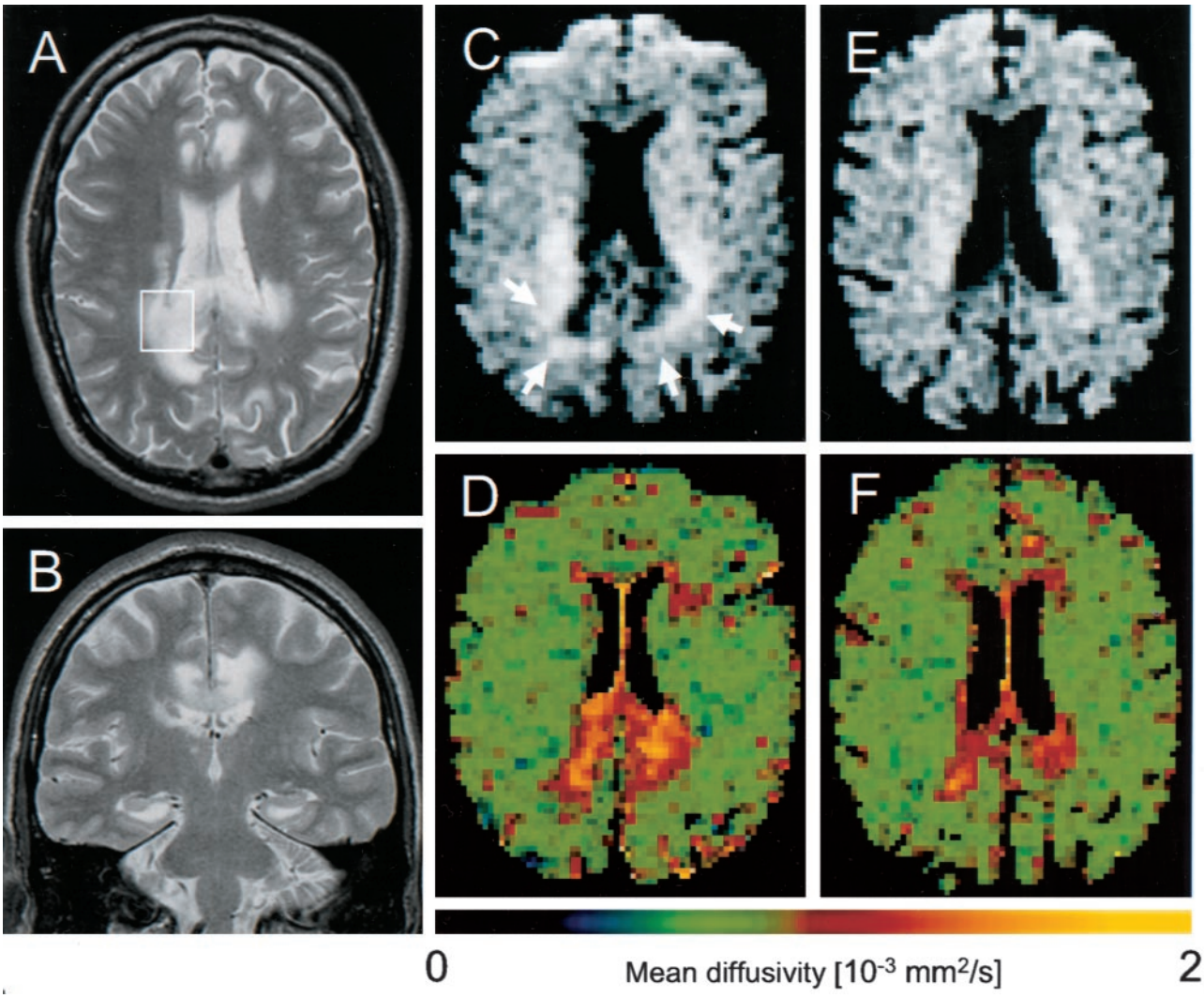

FIG 1. *A* and *B,* Axial and coronal T2-weighted images (1.5 T, TR/TE = 3800/84 and 3500/75, respectively) show extensive areas of abnormally high signal intensity in the splenium and the perispenial, cingulate, and the bilateral perisplenial white matter. Note sparing of the hippocampi and the temporal and insular cortices. *C–F,* Diffusion-weighted images (*upper row* [*C* and *E*]) and corresponding apparent diffusion coefficient false-color maps (*lower row*) of week 8 (*D*) and week 26 (*F*) after disease onset. Note that the CSF signal intensity is nulled. *C* and *D,* Lesions on diffusion-weighted images 4 weeks after the first MR study (*C*) show hypointense central area with a hyperintense rim (*arrows*) and high regional mean diffusivity. *E* and *F,* Note resolution of diffusion-weighted hyperintensities and peripheral normalization of regional mean diffusivity, indicating irreversible necrosis and gliosis formation in areas with regional mean diffusivity exceeding about 1.4 $\times 10^{-3}$ mm^2/s, whereas initially hyperintense areas on diffusion-weighted images, mainly representing T2 shine-through, without corresponding reduction of regional mean diffusivity reflect potentially reversible inflammatory changes. (Image acquisition: TR/TE = 2200/120, tetrahedral gradient acquisition scheme [15] with b values of 330, 798, and 1320 s/mm^2)

Despite treatment that included antiretroviral therapy, foscarnet, methadon substitution, and antipsychotic medication for increasing delirium, the clinical course deteriorated and led to repeat lumbar puncture that disclosed a positive PCR result for HSV. Findings for VZV, CMV, and JC virus remained negative. In week 7 after the onset of symptoms, stereotactic biopsy of the left cingulate gyrus was performed, and histopathologic examination confirmed the diagnosis of necrotizing HSV encephalitis with prominent gliotic reaction (Fig 3).

The patient began a 2-week course of intravenous acyclovir (3×80 mg/day) that resulted in immediate improvement of his mental status. After 5 days, MR imaging showed slightly reduced mass effect and better demarcation of most of the lesions, whereas both internal capsular hyperintensities had expanded. On diffusion-weighted images, the perisplenial and cingulate lesions were hypointense with hyperintense rims (Fig 1C); for the other T2 lesions, no corresponding signal intensity alterations were detectable. Regional mean diffusivity was elevated by between 33% and 97% within five different lesions compared with that of normal-appearing right frontal white matter (Fig 1D*;* Table).

Eighteen weeks later, CSF PCR findings for HSV were negative. MR imaging showed focal atrophy of the splenium and regression of all lesions including the capsular, occipital, and cerebellar abnormalities. Regional mean diffusivity within all measured lesions was less elevated (Fig 1F*;* Table). Both follow-up spectra showed a partial recovery of NAA; an increase in mI most pronounced in the 26th week; partial normalization of elevated Cho, Lip, and Lac; and complete normalization of Cr (Fig 2). Up to this point, the patient made a partial recovery but still had residual mild hemiparesis, depressive syndrome, and severe cognitive impairment.

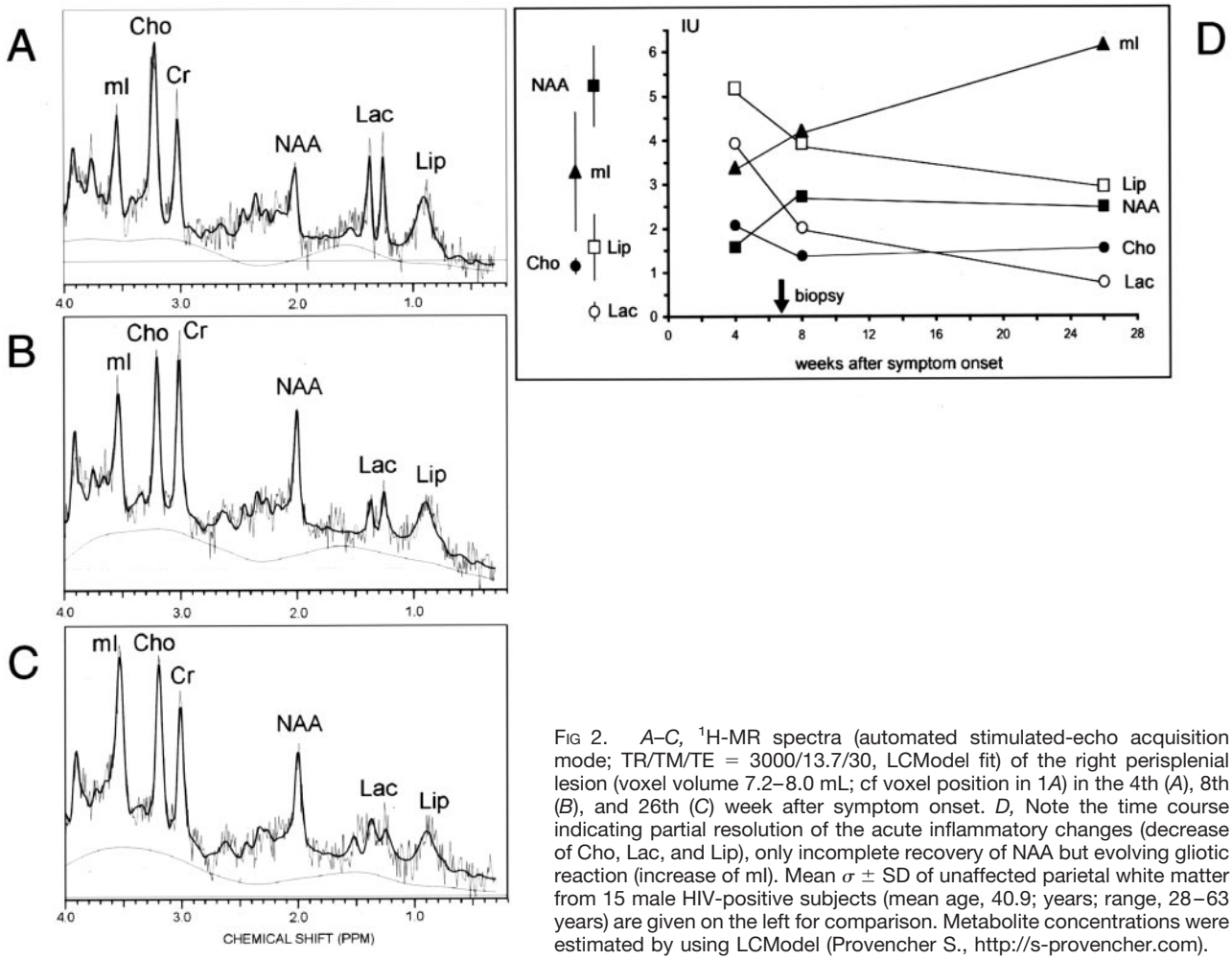

FIG 2. *A–C,* ^{1}H-MR spectra (automated stimulated-echo acquisition mode; TR/TM/TE = 3000/13.7/30, LCModel fit) of the right perisplenial lesion (voxel volume 7.2–8.0 mL; cf voxel position in 1*A*) in the 4th (*A*), 8th (*B*), and 26th (*C*) week after symptom onset. *D,* Note the time course indicating partial resolution of the acute inflammatory changes (decrease of Cho, Lac, and Lip), only incomplete recovery of NAA but evolving gliotic reaction (increase of mI). Mean $\sigma \pm$ SD of unaffected parietal white matter from 15 male HIV-positive subjects (mean age, 40.9; years; range, 28–63 years) are given on the left for comparison. Metabolite concentrations were estimated by using LCModel (Provencher S., http://s-provencher.com).

Discussion

Using MR imaging and ^{1}H-MRS, we demonstrated a multifocal necrotizing inflammation that involved mainly both cingulate and parahippocampal gyri, the splenium, and the perisplenial regions. Contrary to extensively studied sporadic HSE, the hippocampi as well as the frontobasal, insular, and temporal cortices were spared, while white matter was predominantly affected, and occipital and exceptional cerebellar lesions were present (7). This pattern suggests that HIV infection can distinctly modify the spatial distribution of HSE as compared with immunocompetent adults. Our case would thus add to previous reports on atypical HIV-related clinicopathologic presentations, including myelitis, brain stem encephalitis, ventriculoencephalitis, and focal parenchymal encephalitis without further topographic classification (1–3).

The metabolic alterations of our case (Fig 2) correspond well with the histopathologic findings and reported ^{1}H-MR spectra of non-HIV-related HSE using only long echo times: NAA was consistently reduced between 7 and 14 weeks after onset, whereas elevated Cho was observed in four of six cases and Lac in one case (8–11). These changes are thought to reflect neuronal or axonal injury (NAA), demyelination (Cho, Lip) and anaerobic metabolism, or presence of macrophages (Lac).

Histopathologic examination depicted necrosis (Fig 3A) with loss of neurons and axons, macrophage infiltration (Fig 3B and C), and prominent gliosis with reactive astrocytosis (Fig 3C and D). Glial proliferation in HIV-related HSE as such has been observed post mortem (2) and, intriguingly, was associated with progressive mI increase along with complete or partial normalization of the other metabolites in our case. To compensate for other HIV-related metabolic alterations, we compared the individual course with that in a group of male HIV patients lacking focal disease. The regression of elevated Cho, Lip, and Lac first seen in the 8th week complies well with the clinical improvement, radiologic lesion resolution, and negative follow-up CSF PCR findings for HSV. Our observation of the NAA recovery paralleling improvement of neurologic function is consistent with transient decreases observed in HSE (8, 10) and other diseases.

Diffusion-weighted imaging and mean diffusivity analysis revealed different lesion types: The perisplenial and cingulate lesions showed peripherally high diffusion signal intensity, mainly representing T2 shine-through, and central high mean diffusivity with

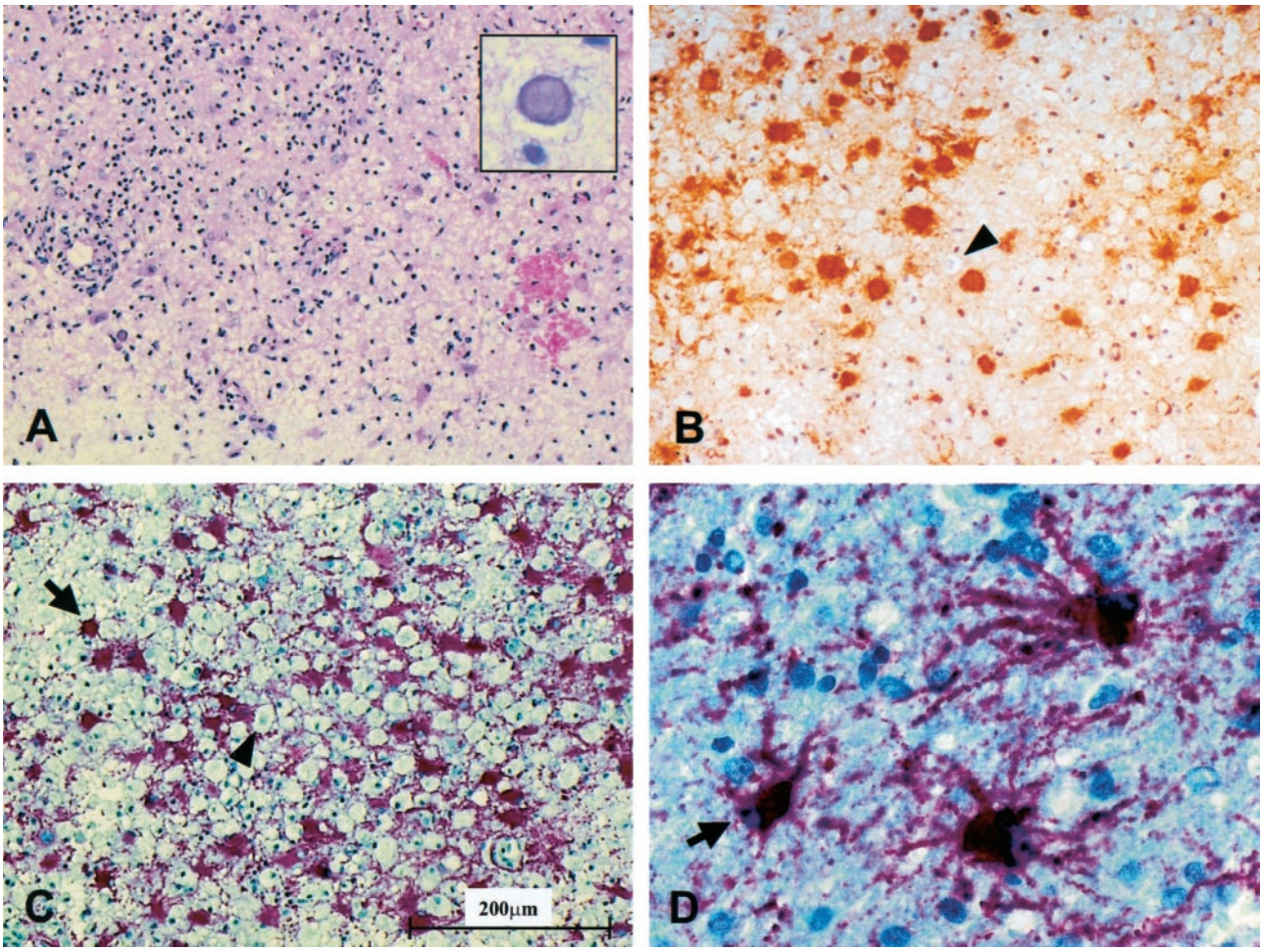

FIG 3. Histopathologic examination of the biopsies of the left cingulate gyrus revealed the morphology of a hemorrhagic-necrotizing inflammation (*A,* [H&E staining]) with multiple cells containing Cowdry type A intranuclear inclusions (*insert*). Immunohistochemical detection of HSV antigen is depicted in *B.* By using an antibody directed against the glial fibrillary acid protein, a prominent gliosis with multiple reactive astrocytes (*C* and *D*) intermixed with macrophages (*B* and *C*) could be detected. Astrocytes and macrophages are marked by *arrows* and *arrowheads,* respectively.

Regional Mean Diffusivity (D) in the 8th and 26th Week

Region	Mean diffusivity D ($\times 10^{-3}$ mm^2/s; mean ± SD [% relative to control])	
	8th week	26th week
Right frontal white matter (control)	0.672 ± .094 (100)	0.722 ± .089 (100)
Left perisplenial	1.258 ± .214 (187)	1.177 ± .108 (163)
Right perisplenial	1.084 ± 0.283 (161)	1.232 ± .215 (171)
Left cingulate	1.038 ± .217 (154)	0.995 ± .141 (138)
Left parahippocampal	0.920 ± .158 (137)	0.771 ± .110 (107)
Right parahippocampal	0.843 ± .121 (125)	0.788 ± .101 (109)

Note—Numbers in parentheses are percentages.

minor reduction at follow-up. This may indicate severe and potentially irreversible tissue destruction (eg, central necrosis or gliosis formation with peripheral transient cell infiltration). In contrast, the parahippocampal lesions showed subtotal resolution of the T2 lesions, no hyperintense signal on diffusion-weighted images, and less mean diffusivity elevation that nearly normalized. These findings suggest involution of vasogenic edema and probably demyelinating rather than destructive tissue disease which supports the diagnostic potential of mean diffusivity as a tool to classify the severity of inflammatory brain lesions. Furthermore, during the acute stages of HSE, reduced diffusivity has been reported (7, 12), which may characterize the most severe tissue damage being associated with poor clinical outcome (12).

The histopathologic findings, together with CSF PCR and the radiologic course, strongly support that HSV type 1 was the main pathologic agent in the reported patient. Both CMV and VZV were not detectable by means of PCR in two CSF samples; furthermore, concomitant CMV encephalitis, which is seen in most HIV-related HSE (1–3), could not be verified by immunohistochemistry. PML was not definitely excluded by immunohistochemistry but seems unlikely in view of a survival time of 52 months without progressive focal symptoms and repeated negative PCR findings for JC virus. In light of the reported metabolic changes of subacute PML lesions (4), the metabolic profile of

this case could not be clearly distinguished; however, the initial NAA and Cho changes were larger as were the mean diffusivity elevations compared with reported regional mean diffusivity of subacute PML lesions (5), probably reflecting differences in the severity of individual tissue reaction rather than their different causes. This interpretation is in line with MRS findings in a demyelinating plaque (13) and with a report on five biopsy-diagnosed nonneoplastic cerebral lesions misclassified as neoplastic based on "typical" spectroscopic profiles (14)—ie, elevated Cho and decreased NAA and Cr with or without detectable mobile lipids and Lac. These cases, representing fulminant demyelination and chronic human herpesvirus 6 encephalitis, all showed an extensive inflammatory cell infiltrate and varying degrees of gliosis as rather unspecific pathologic findings similar to those in our case. In conjunction with standard and diffusion imaging and very little space-occupying effect, necrosis, and minor cellular density, the observed metabolic pattern was indicative of necrotizing encephalitis and clearly distinguishable from tumors. Moreover, accumulation of mobile lipids, especially resonating at 1.3 ppm, is suggestive of high-grade malignancy (14), but typically associated either with a higher Cho-Cr ratio or a global strong reduction of Cho, Cr, and NAA.

Conclusion

By delivering insight into the time course of the metabolic and ultrastructural tissue pathology, ^{1}H-MRS and diffusion-weighted imaging confirmed that an intact cell-mediated immune response is not a prerequisite for necrotizing HSE with marked inflammatory and glial reaction. Regarding clinical care, both modalities helped to redirect attention to necrotizing encephalitis in a situation in which a broad range of potential opportunistic abnormalities, initial inconclusive microbiologic screening, and a protracted clinical course were distractions from the diagnosis of HSE.

References

1. Schiff D, Rosenblum MK. **Herpes simplex encephalitis (HSE) and the immunocompromised: a clinical and autopsy study of HSE in the settings of cancer and human immunodeficiency virus-type 1 infection.** *Hum Pathol* 1998;29:215–222
2. Chretien F, Belec L, Hilton DA, et al. **Herpes simplex virus type 1 encephalitis in acquired immunodeficiency syndrome.** *Neuropathol Appl Neurobiol* 1996;22:394–404
3. Cinque P, Vago L, Marenzi R, et al. **Herpes simplex virus infections of the central nervous system in human immunodeficiency virus-infected patients: clinical management by polymerase chain reaction assay of cerebrospinal fluid.** *Clin Infect Dis* 1998;27:303–309
4. Chang L, Ernst T, Tornatore C, et al. **Metabolite abnormalities in progressive multifocal leukoencephalopathy by proton magnetic resonance spectroscopy.** *Neurology* 1997;48:836–845
5. Chang L, Ernst T. **MR spectroscopy and diffusion-weighted MR imaging in focal brain lesions in AIDS.** *Neuroimaging Clin N Am* 1997;7:409–426
6. Simone IL, Federico F, Tortorella C, et al. **Localised ^{1}H-MR spectroscopy for metabolic characterisation of diffuse and focal brain lesions in patients infected with HIV.** *J Neurol Neurosurg Psychiatry* 1998;64:516–523
7. Ohta K, Funaki M, Tanaka M, Suzuki N. **Early cerebellar involvement on diffusion- weighted magnetic resonance images in herpes simplex encephalitis.** *J Neurol* 1999;246:736–738
8. Menon DK, Sargentoni J, Peden CJ, et al. **Proton MR spectroscopy in herpes simplex encephalitis: assessment of neuronal loss.** *J Comput Assist Tomogr* 1990;14:449–452
9. Demaerel P, Wilms G, Robberecht W, et al. **MRI of herpes simplex encephalitis.** *Neuroradiology* 1992;34:490–493
10. Takanashi J, Sugita K, Ishii M, et al. **Longitudinal MR imaging and proton MR spectroscopy in herpes simplex encephalitis.** *J Neurol Sci* 1997;149:99–102
11. Hitosugi M, Ichijo M, Matsuoka Y, et al. **Proton MR spectroscopy findings in herpes simplex encephalitis.** *Clin Neurol* 1996;36:839–843
12. Sener RN. **Herpes simplex encephalitis: diffusion MR imaging findings.** *Comput Med Imaging Graph* 2001;25:391–397
13. Arnold DL, Matthews PM, Francis GS, et al. **Proton magnetic resonance spectroscopic imaging for metabolic characterization of demyelinating plaques.** *Ann Neurol* 1992;31:235–241
14. Krouwer HGJ, Kim TA, Rand SD, et al. **Single-voxel proton MR spectroscopy of nonneoplastic brain lesions suggestive of a neoplasm.** *AJNR Am J Neuroradiol* 1998;19:1695–1703
15. Conturo TE, McKinstry RC, Akbudak E, Robinson BH. **Encoding of anisotropic diffusion with tetrahedral gradients: a general mathematical diffusion formalism and experimental results.** *Magn Reson Med* 1996;35:399–412